Structural Distortion of 6-Coordinated Fe(II) Complexes in Zeolite Y

Yasushi Umemura*

Department of Chemistry, National Defense Academy, Yokosuka, Kanagawa 239, Japan

Yoshitaka Minai

Center for Arts and Sciences, Musashi University, Nerima-ku, Tokyo 176, Japan

Takeshi Tominaga

School of Science, University of Tokyo, Bunkyo-ku, Tokyo 113, Japan

Received: January 6, 1998; In Final Form: September 29, 1998

Six-coordinated Fe(II) complex ions $[FeL_3]^{2+}$ (L = en, amp, bpy, dmbpy, phen, and dmphen), prepared in a supercage of zeolite Y, were characterized by UV−vis, XRD, Mössbauer spectroscopy, and IR. The UV−vis spectra and XRD patterns of the zeolite encapsulating the Fe(II) complex ions show that $[Fe(en)_3]^{2+}$, $[Fe(amp)_3]^{2+}$, $[Fe(bpy)_3]^{2+}$, and $[Fe(phen)_3]^{2+}$ are formed in the zeolite supercage. The Mössbauer spectra of $[Fe(bpy)_3]^{2+}$ and $[Fe(phen)_3]^{2+}$ in the supercage gave extraordinarily large values of the quadrupole splitting for low-spin Fe(II) species, indicating that these complex ions in a supercage are distorted by a strong steric interaction with the zeolite lattice. The IR spectra of $[Fe(bpy)_3]^{2+}$ and $[Fe(phen)_3]^{2+}$ in the supercage as well as their Mössbauer results reveal that the complex ion is located in the supercage; (i) the 3-fold axis of the complex is parallel to that of the supercage, (ii) each of the three bidentate-ligand molecules in the complex faces to the 12-membered ring of the supercage, and (iii) the complex is twisted around its 3-fold axis toward a trigonal prism.

Introduction

During the last few decades, intrazeolite chemistry has attracted the attention of many scientists who have been applying compounds in a zeolite cage for catalysis and gas purification,[1,2] for example. A molecule encapsulated in a zeolite cage is characterized by a steric restriction, isolation from other molecules by the zeolite lattice,[3] and low mobility.[4] Besides, if the size of the molecule is comparable to that of the zeolite cage, the molecule may suffer a strong steric restriction in the cage. In such a case, the molecule in the cage may show interesting properties, which are not seen under ordinary conditions. It is very important to investigate the steric restriction of a molecule in a zeolite cage; there have been many reports[5−19] on this subject. However, it is noteworthy that most reports have dealt with a steric restriction of molecules that are smaller than the zeolite cages.

The supercage of zeolite Y is about 13 Å in diameter. The spectroscopic characteristics and reactivities[5,20−23] of some complexes, such as $[Ru(bpy)_3]^{2+}$ [3,4,24−27] and [Co(salen)], [28−31] in the supercage of zeolite Y have been investigated. The complexes often exhibit novel properties, perhaps depending on their location in the cage and degree of distortion. Some schematic models[2,16,22,28] for distorted complexes in a zeolite cage have been proposed on the basis of a computer calculation.

It is well-known that Mössbauer spectroscopy is useful to characterize such elements such as iron, even in noncrystalline or amorphous materials, and that any impurities other than iron type never affect the features in the Mössbauer spectrum. Thus, Mössbauer spectroscopy is regarded as being one of the most suitable techniques which can be used to investigate the chemical state of iron atoms or ions included in zeolite.[5,32−35]

In this study we prepared Fe(II) complex ions $[FeL_3]^{2+}$ with various volumes (L = en, 1,2-diaminoethane; amp, 2-(aminomethyl)pyridine; bpy, 2,2′-bipyridine; dmbpy, 4,4′-dimethyl-2,2′-bipyridine; phen, 1,10-phenanthroline; and dmphen, 5,6-dimethyl-1,10-phenanthroline) in a supercage of zeolite Y. The degree of distortion and the location of $[Fe(bpy)_3]^{2+}$ and $[Fe(phen)_3]^{2+}$ in zeolite Y[36] have been verified by means of Mössbauer and infrared spectroscopies.

Experimental Section

Sodium-substituted zeolite Y, (Na^+−Y, SK-40), was purchased from Nikka Seiko Co., and $FeSO_4 \cdot 7H_2O$ and $FeCl_2 \cdot nH_2O$ (n= 4−6) (for quantitative analysis) were obtained from Wako Chemicals. Water boiled for a few hours was cooled to room temperature with the bubbling of nitrogen gas before acidification to pH 1−2 with a few drops of concentrated HCl aqueous solution, just prior to use. Methanol was deoxygenated by bubbling nitrogen gas for a few hours. All manipulations were performed under nitrogen.

$[Fe(en)_3]^{2+}$/Zeolite. $[Fe(en)_3]^{2+}$ included in zeolite Y is denoted by $[Fe(en)_3]^{2+}$/zeolite; similar denotations are used hereafter.

Dried methanol was used for preparing the complex in zeolite Y because $[Fe(en)_3]^{2+}$ can be easily oxidized and hydrolyzed by a trace of water. Four grams of Na^+−Y zeolite dried at 150 °C for several days and at 400 °C for 2 h in vacuo was suspended in 200 mL of a methanolic $FeCl_2$ solution (0.02 mol/

* To whom correspondence should be addressed. E-mail: umemura@cc.nda.ac.jp.

10.1021/jp980663r CCC: $18.00
Published on Web 01/13/1999

L) for 1 day. After the zeolite was separated from the solution, it was washed with a large amount of methanol to obtain Fe^{2+}−Y zeolite. The Fe^{2+}−Y zeolite was suspended in 250 mL of a methanolic solution of anhydrous 1,2-diaminoethane (0.03 mol/L) for 1 day. The zeolite separated from the solution was washed with a large amount of methanol containing a small portion of diaminoethane to obtain $[Fe(en)_3]^{2+}$/zeolite. Elemental analysis has shown that $[Fe(en)_3]^{2+}$/zeolite included 1.2 iron atoms per supercage.

$[Fe(amp)_3]^{2+}$/Zeolite. Fe^{2+}−Y zeolite was prepared by suspending 6 g of Na^+−Y zeolite in 500 mL of an aqueous $FeSO_4$ solution (0.1 mol/L) and washing the zeolite with a large amount of water after filtration. The Fe^{2+}−Y zeolite was suspended in 125 mL of an aqueous 2-(aminomethyl)pyridine (amp) solution (0.4 mol/L) for 1 day, and the aqueous solution was removed. After being washed with some amounts of water containing a small portion of amp, the zeolite was suspended in 125 mL of an aqueous NaCl solution (0.4 mol/L) with a trace of amp for 1 day in order to exchange any noncoordinated iron ions in the zeolite for sodium ions. The zeolite was separated by filtration and washed with a large amount of water containing amp until the filtrate became colorless. $[Fe(amp)_3]^{2+}$/zeolite contained 1.9 iron atoms per supercage.

$[Fe(bpy)_3]^{2+}$/Zeolite and $[Fe(phen)_3]^{2+}$/Zeolite. Six grams of Fe^{2+}−Y zeolite prepared similarly to the procedure described above was suspended in 250 mL of an aqueous solution of each ligand (saturated for 2,2′-bipyridine and 0.02 mol/L for 1,10-phenanthroline) for 1 day. After separation by filtration and washing with a large amount of water, the zeolite was suspended in 250 mL of an aqueous NaCl solution (1 mol/L) for 1 day. The zeolite was filtered off and washed with a large amount of water until the filtrate became colorless and was succeedingly washed with methanol by a Soxhlet extraction method for a few days. After drying in vacuo, $[Fe(bpy)_3]^{2+}$/zeolite and $[Fe(phen)_3]^{2+}$/zeolite containing 0.43 and 0.47 iron atoms per supercage, respectively, were obtained.

$[Fe(dmbpy)_3]^{2+}$/Zeolite and $[Fe(dmphen)_3]^{2+}$/Zeolite. Two grams of Fe^{2+}−Y zeolite prepared in a methanolic $FeCl_2$ solution was suspended for 1 day in 250 mL of a methanolic 4,4′-dimethyl-2,2′-bipyridine solution (0.03 mol/L) or in 100 mL of a methanolic 5,6-dimethyl-1,10-phenanthroline solution (5 mmol/L). After removing the methanolic solution and washing with methanol, the zeolite was suspended in 100 mL of a methanolic NaBr solution (1 mol/L) for 1 day. The zeolite separated from the solution was washed with a large amount of methanol until the filtrate became colorless. The zeolite was dried in vacuo to obtain $[Fe(dmbpy)_3]^{2+}$/zeolite and $[Fe(dmphen)_3]^{2+}$/zeolite.

Corresponding Polycrystalline Complexes. Corresponding polycrystalline complexes were synthesized according to procedures described in the literature.[37−39]

X-ray Diffraction and Spectroscopic Methods. X-ray diffraction (XRD) patterns were recorded under ambient atmosphere with a Rigaku RAD-1A diffractometer using Ni-filtered Cu Kα radiation.

The ultraviolet−visible (UV−vis) spectra were recorded with a Hitachi U-3500 spectrophotometer. The transmission spectra of the solutions or suspensions were measured by a conventional method with a 1 cm length cell. Diffuse reflectance spectra were recorded using an integrating sphere attachment (6 cm in diameter) with barium sulfate powder as a reference. The Kubelka−Munk function was not applied to the diffuse reflectance spectra, because of the winding base lines. Instead,

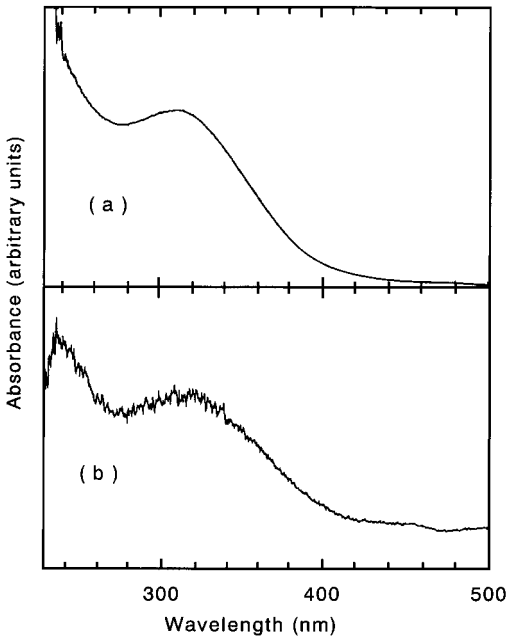

Figure 1. UV−vis spectra of (a) methanolic $[Fe(en)_3](ClO_4)_2$ solution and (b) suspension of $[Fe(en)_3]^{2+}$/zeolite in methanol.

logarithmic relative reflectivity,

$$-\log(r) = -\log[R_{\text{sample}}/R_{\text{reference}}]$$

was employed.

The Mössbauer spectra were measured with an Austin S-600 Mössbauer spectrometer. The samples were kept at 78 K in a specially designed cryostat during the measurement. Iron foil (α-iron) was used as a standard for energy calibration. The spectra were deconvoluted to multiple Lorentzian curves by a least-squares-fitting routine.

The infrared (IR) spectra were obtained with a JEOL JIR-5500 Fourier transform infrared spectrophotometer.

Results and Discussion

The UV−vis spectra of a methanolic $[Fe(en)_3](ClO_4)_2$ solution and of a suspension of $[Fe(en)_3]^{2+}$/zeolite in methanol are shown in Figure 1. The spectrum of $[Fe(en)_3](ClO_4)_2$ (Figure 1a) has a contour with an absorption maximum at around 320 nm. A similar contour is observed in the spectrum of a $[Fe(en)_3]^{2+}$/zeolite suspension (Figure 1b). The UV−vis spectrum of a filtrate of the suspension of $[Fe(en)_3]^{2+}$/zeolite through a membrane filter (pore diameter: 0.45 μm) shows no absorption: it is likely that the absorption seen in the spectrum of the suspension is due to $[Fe(en)_3]^{2+}$ in zeolite Y. Therefore, $[Fe(en)_3]^{2+}$ may have been formed in the zeolite cage.

The UV−vis spectrum of a methanolic $[Fe(bpy)_3]Cl_2{\cdot}7H_2O$ solution and the diffuse reflectance UV−vis spectrum of $[Fe(bpy)_3]^{2+}$/zeolite are shown in Figure 2. The spectrum of $[Fe(bpy)_3]^{2+}$/zeolite (Figure 2b) is identical to that of the methanolic $[Fe(bpy)_3]Cl_2{\cdot}7H_2O$ solution (Figure 2a), suggesting that $[Fe(bpy)_3]^{2+}$ is encapsulated in the zeolite cage.

The UV−vis spectrum of a suspension of $[Fe(amp)_3]^{2+}$/zeolite in methanol and the reflectance spectrum of $[Fe(phen)_3]^{2+}$/zeolite are also very similar to those of methanolic $[Fe(amp)_3](ClO_4)_2$ and methanolic $[Fe(phen)_3]Cl_2{\cdot}7H_2O$ solutions, respectively. Those results show that $[Fe(amp)_3]^{2+}$ and $[Fe(phen)_3]^{2+}$ are formed in the supercage. However, $[Fe(dmbpy)_3]^{2+}$/zeolite and $[Fe(dmphen)_3]^{2+}$/zeolite have no absorption maxima in the UV−vis region,[24] while the UV−vis spectra of methanolic

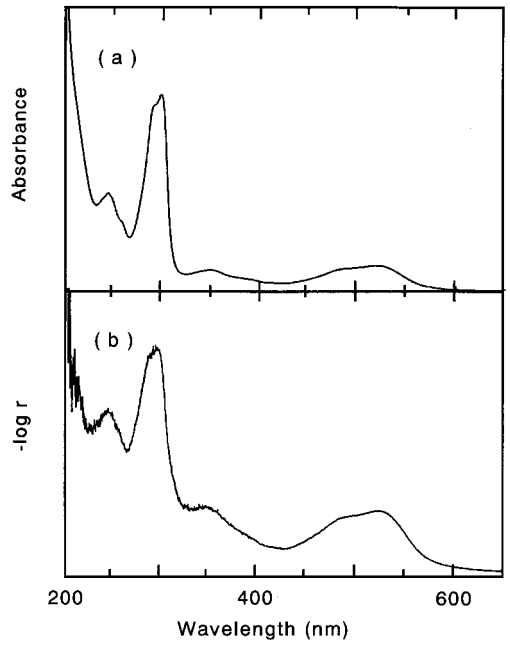

Figure 2. UV−vis spectra of (a) methanolic $[Fe(bpy)_3]Cl_2 \cdot 7H_2O$ solution and (b) $[Fe(bpy)_3]^{2+}$/zeolite (diffuse reflectance).

$[Fe(dmbpy)_3](ClO_4)_2$ and methanolic $[Fe(dmphen)_3](ClO_4)_2$ solutions have absorption maxima, indicating that $[Fe(dmbpy)_3]^{2+}$ and $[Fe(dmphen)_3]^{2+}$ may not be able to exist in the supercage.

These UV−vis spectral data suggest that $[Fe(en)_3]^{2+}$, $[Fe(amp)_3]^{2+}$,$[Fe(bpy)_3]^{2+}$, and $[Fe(phen)_3]^{2+}$ are formed in the supercage of zeolite Y. However, there still remains a possibility that these complex ions are strongly adsorbed on the external surface or mesopore of the zeolite particles.

Quayle and co-workers[4,5] reported that the formation of a large transition-metal complex ion in the supercage of zeolite Y could be confirmed by the change in the relative peak intensities of 220 and 311 reflections in the XRD pattern: $I_{220} > I_{311}$ for zeolite Y and $I_{220} < I_{311}$ for the zeolite including the large complex ion. This empirical relationship among the XRD intensities may be related to the distribution of noncoordinated free cations in zeolite Y.[4,5]

Figure 3 shows XRD patterns of Fe^{2+}−Y zeolite, $[Fe(bpy)_3]^{2+}$ ion adsorbed on the external surface or mesopore of zeolite Y, which was prepared by immersion in an aqueous $[Fe(bpy)_3]Cl_2$ solution, and $[Fe(bpy)_3]^{2+}$/zeolite. The 220 and 311 reflections are seen at $2\theta = 10$ and 12°, respectively. I_{220} is higher than I_{311} in both the XRD patterns of Fe^{2+}−Y zeolite and Na^{+}−Y zeolite adsorbing $[Fe(bpy)_3]^{2+}$ on the external surface (Figure 3a and b), whereas I_{220} is lower than I_{311} for $[Fe(bpy)_3]^{2+}$/zeolite (Figure 3c). Similar changes in the intensities of the 220 and 311 reflections are observed for $[Fe(en)_3]^{2+}$/zeolite, $[Fe(amp)_3]^{2+}$/zeolite, and $[Fe(phen)_3]^{2+}$/zeolite. However, the relative intensities are not changed in the XRD patterns of $[Fe(dmbpy)_3]^{2+}$/zeolite and $[Fe(dmphen)_3]^{2+}$/zeolite. Therefore, the supercage of $[Fe(en)_3]^{2+}$/zeolite, $[Fe(amp)_3]^{2+}$/zeolite, $[Fe(bpy)_3]^{2+}$/zeolite, and $[Fe(phen)_3]^{2+}$/zeolite would accommodate the corresponding complex ions. This result is consistent with that obtained from the UV−vis spectral analysis.

The Mössbauer spectra of polycrystalline $[Fe(en)_3](ClO_4)_2$ and $[Fe(en)_3]^{2+}$/zeolite are shown in Figure 4. The Mössbauer spectrum of $[Fe(en)_3](ClO_4)_2$ gives a high-spin doublet (isomer shift, IS = 1.09 mm/s; quadrupole splitting, QS = 1.73 mm/s), ascribed to Fe^{2+} ions in $[Fe(en)_3](ClO_4)_2$, together with a doublet for the Fe^{3+} impurities (Figure 4a). The Mössbauer spectrum

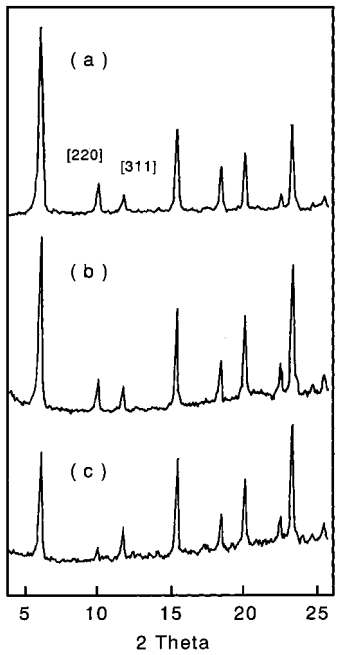

Figure 3. XRD patterns of (a) Fe^{2+}−Y zeolite, (b) $[Fe(bpy)_3]^{2+}$ on the surface of Na^{+}−Y zeolite, and (c) $[Fe(bpy)_3]^{2+}$/zeolite.

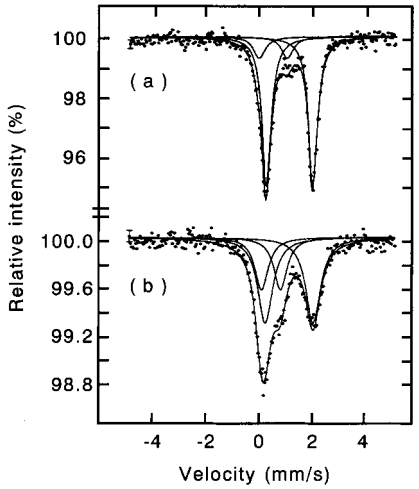

Figure 4. Mössbauer spectra of (a) $[Fe(en)_3](ClO_4)_2$ and (b) $[Fe(en)_3]^{2+}$/zeolite recorded at 78 K.

of $[Fe(en)_3]^{2+}$/zeolite indicates a doublet with Mössbauer parameters similar to those for $[Fe(en)_3](ClO_4)_2$ (IS = 1.11 mm/s and QS = 1.77 mm/s), although the line widths of the doublet are broader and the other doublet for the Fe^{3+} impurities is rather intense.

$[Fe(amp)_3](ClO_4)_2$ behaves as a spin−crossover complex with high spin at room temperature and low spin at 78 K.[38,40−43] The spin−crossover behavior of $[Fe(amp)_3]^{2+}$ in zeolite Y was reported in a preliminary communication.[44] The Mössbauer spectrum of $[Fe(amp)_3]^{2+}$/zeolite recorded at 78 K gives a singlet (IS = 0.57 mm/s) attributed to Fe^{2+} ions in low-spin fac-$[Fe(amp)_3]^{2+}$. On the other hand, fac-$[Fe(amp)_3](ClO_4)_2$ [45] exhibits a singlet (IS = 0.52 mm/s) in its Mössbauer spectrum recorded at 78 K. The Mössbauer parameter for fac-$[Fe(amp)_3](ClO_4)_2$ is identical to that for the singlet observed in the Mössbauer spectrum of $[Fe(amp)_3]^{2+}$/zeolite. The Mössbauer spectrum of fac-$[Fe(amp)_3](ClO_4)_2$ recorded at 293 K indicates an asymmetric doublet ascribed to Fe^{2+} ions in high-spin fac-$[Fe(amp)_3]^{2+}$. An identical component is also observed in the

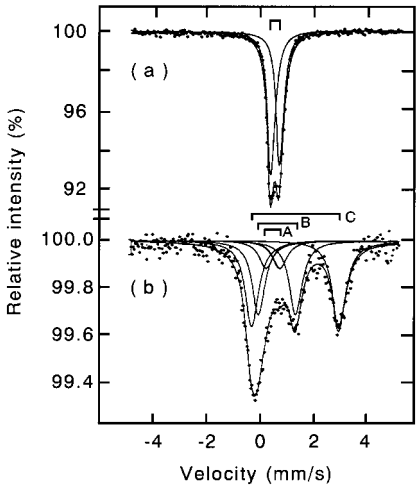

Figure 5. Mössbauer spectra of (a) $[Fe(bpy)_3]Cl_2 \cdot 7H_2O$ and (b) $[Fe(bpy)_3]^{2+}$/zeolite recorded at 78 K.

TABLE 1: Mössbauer Parameters at 78 K for $[FeL_3]^{2+}$ Salts and $[FeL_3]^{2+}$ Ions Encapsulated in Zeolite Y and Fe(II)−H Distances for $[FeL_3]^{2+}$ Ions

	IS (mm/s)[a]	QS (mm/s)	Fe(II)-H distance (Å)[c]
$[Fe(en)_3](ClO_4)_2$	1.09(0)[b]	1.73(0)	
$[Fe(en)_3]^{2+}$ in zeolite Y	1.11(2)	1.77(3)	3.7
fac-$[Fe(amp)_3](ClO_4)_2$	0.52(0)		
fac-$[Fe(amp)_3]^{2+}$ in zeolite Y	0.57(1)		5.7[d]
$[Fe(bpy)_3]Cl_2 \cdot 7H_2O$	0.39(0)	0.32(0)	
$[Fe(bpy)_3]^{2+}$ in zeolite Y	0.54(1)	1.39(1)	5.8
$[Fe(phen)_3]Cl_2 \cdot 7H_2O$	0.40(1)	0.26(2)	
$[Fe(phen)_3]^{2+}$ in zeolite Y	0.54(1)	1.41(1)	6.3
$[Fe(dmbpy)_3]^{2+}$			6.6
$[Fe(dmphen)_3]^{2+}$			7.3

[a] Relative to α-iron. [b] Digits in parentheses indicate standard deviations of the parameters. [c] A computer calculated distance from an Fe(II) ion to the farthest hydrogen atom in each complex. [d] A shape of amp is asymmetric. A distance from an Fe(II) ion to an ethylene proton is 3.6 Å.

Mössbauer spectrum of $[Fe(amp)_3]^{2+}$/zeolite recorded at the same temperature.

Figure 5 shows the Mössbauer spectra of $[Fe(bpy)_3]Cl_2 \cdot 7H_2O$ and $[Fe(bpy)_3]^{2+}$/zeolite.[5] The spectrum of $[Fe(bpy)_3]Cl_2 \cdot 7H_2O$ indicates a low-spin doublet (IS = 0.39 and QS = 0.32 mm/s) assigned to Fe^{2+} in the polycrystalline complex (Figure 5a). The spectrum of $[Fe(bpy)_3]^{2+}$/zeolite comprises three doublets, denoted by A, B, and C in order of increasing quadrupole splitting (Figure 5b). Doublets A and C correspond to the doublets in the Mössbauer spectrum of Fe^{2+}−Y zeolite containing Fe^{3+} as impurities measured at 78 K. Therefore, doublets A and C are attributable to free iron ions: Fe^{3+} and Fe^{2+} in zeolite Y, respectively. Thus, the remaining doublet B in the spectrum of $[Fe(bpy)_3]^{2+}$/zeolite can be assigned to Fe^{2+} ions in $[Fe(bpy)_3]^{2+}$ in the supercage. Doublet B indicates a much larger quadrupole splitting than that of $[Fe(bpy)_3]Cl_2 \cdot 7H_2O$.

The Mössbauer spectral features of $[Fe(phen)_3]Cl_2 \cdot 7H_2O$ and $[Fe(phen)_3]^{2+}$/zeolite[21] are very similar to those of $[Fe(bpy)_3]Cl_2 \cdot 7H_2O$ and $[Fe(bpy)_3]^{2+}$/zeolite.

The Mössbauer parameters of $[Fe(en)_3]^{2+}$, $[Fe(amp)_3]^{2+}$, $[Fe(bpy)_3]^{2+}$, and $[Fe(phen)_3]^{2+}$ in the supercage of zeolite Y and those of the corresponding polycrystalline complexes are listed in Table 1, together with the distance from an Fe(II) ion to the farthest hydrogen atom in each complex ion.

The Mössbauer parameters (IS and QS values) of $[Fe(en)_3]^{2+}$ and $[Fe(amp)_3]^{2+}$ in zeolite Y are close to those of $[Fe(en)_3](ClO_4)_2$ and $[Fe(amp)_3](ClO_4)_2$, respectively. However, the Mössbauer parameters of $[Fe(bpy)_3]^{2+}$, and $[Fe(phen)_3]^{2+}$ in zeolite Y are different from those of $[Fe(bpy)_3]Cl_2 \cdot 7H_2O$ and $[Fe(phen)_3]Cl_2 \cdot 7H_2O$, indicating that these complex ions may suffer a structural deformation in the supercage. The IS values of $[Fe(bpy)_3]^{2+}$ and $[Fe(phen)_3]^{2+}$ in zeolite Y are larger than those of the corresponding polycrystalline complexes, suggesting that the electron density at the iron nucleus decreases along with a decrease in the volume of the complex[46,47] in the cage. Moreover, it is noteworthy that the QS values of $[Fe(bpy)_3]^{2+}$ and $[Fe(phen)_3]^{2+}$ in zeolite Y are extraordinarily large for divalent iron ions in the low spin state. Since the quadrupole splitting depends on the electric field gradient at the iron nucleus, it is sensitive to a structural change from the symmetrical coordination. This implies that $[Fe(bpy)_3]^{2+}$ and $[Fe(phen)_3]^{2+}$ in zeolite Y are largely distorted from the ideal octahedral symmetry by introduction into the supercage.

Since $[Fe(phen)_3]^{2+}$ is larger than $[Fe(bpy)_3]^{2+}$ (Table 1), it is expected that $[Fe(phen)_3]^{2+}$ suffers a larger distortion than

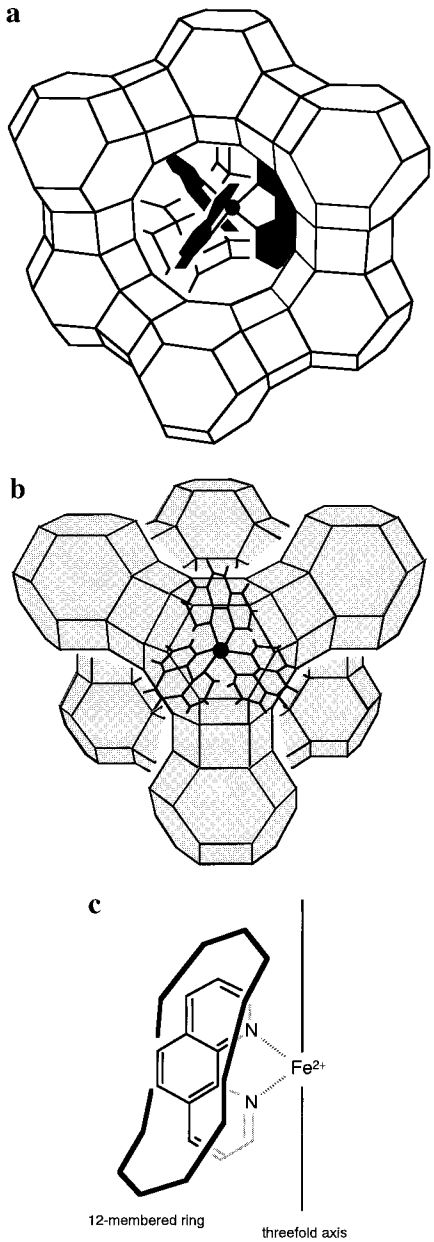

Figure 6. Schematic views of (a and b) $[Fe(phen)_3]^{2+}$ in the supercage and (c) one of the three ligands facing the 12-membered ring of the cage.

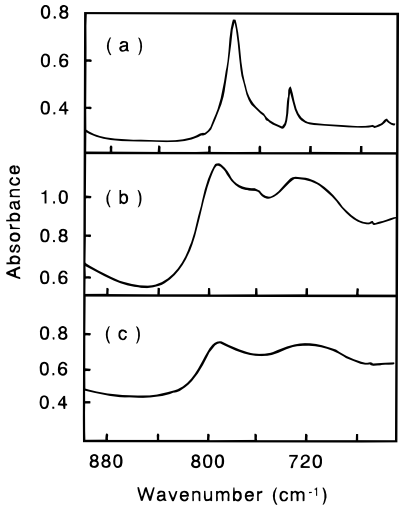

Figure 7. IR spectra of (a) $[Fe(bpy)_3]Cl_2 \cdot 7H_2O$, (b) $[Fe(bpy)_3]^{2+}$/zeolite, and (c) $Fe^{2+}-Y$ zeolite.

does $[Fe(bpy)_3]^{2+}$ in the limited space of the supercage. However, the QS values for $[Fe(bpy)_3]^{2+}$ and $[Fe(phen)_3]^{2+}$ in zeolite Y are identical, implying that $[Fe(bpy)_3]^{2+}$ and $[Fe(phen)_3]^{2+}$ exist in the supercage with a similar degree of distortion. Accordingly, the carbon and hydrogen atoms at the 5- and 6-positions of 1,10-phenanthroline do not influence the steric interaction between the complex and the internal surface of the zeolite.

On the basis of the above discussion, one of the most plausible locations for $[Fe(bpy)_3]^{2+}$ and $[Fe(phen)_3]^{2+}$ in the supercage is as follows (Figure 6a and b for $[Fe(phen)_3]^{2+}$ in the supercage). (i) The 3-fold axis of the complex ion is parallel to the 3-fold axis of the supercage. (ii) Each of the three bidentate-ligand molecules faces toward the 12-membered ring. According to the proposed location, the carbon and hydrogen atoms at the 5- and 6-positions of 1,10-phenanthroline are free from a steric hindrance due to the zeolite lattice.

On the other hand, the carbon and hydrogen atoms at the 4- and 4′-positions in 2,2′-bipyridine and the corresponding 4- and 7-positions in 1,10-phenanthroline would interact with the zeolite lattice effectively, which would lead to a deformation of the complexes in the supercage. This is supported by the fact that $[Fe(dmbpy)_3]^{2+}$ cannot be formed in the supercage, though the size of 4,4′-dimethyl-2,2′-bipyridine is comparable to that of 1,10-phenanthroline (Table 1). The steric effect between the 4- and 4′- methyl groups in 4,4′-dimethyl-2,2′-bipyridine and the zeolite lattice would hinder the formation of $[Fe(dmbpy)_3]^{2+}$ in the supercage.

It is expected from the proposed model of $[Fe(bpy)_3]^{2+}$ and $[Fe(phen)_3]^{2+}$ in the supercage in Figure 6 that (i) two pyridine rings in each of the ligands are under a different environment and that (ii) the complex ion in the cage twists around its 3-fold axis from an octahedron toward a trigonal prism under the influence of the structure of the 12-membered ring.

The IR spectrum for $[Fe(bpy)_3]^{2+}$/zeolite was measured in order to obtain supportive information about the first expectation. The IR spectra of $[Fe(bpy)_3]Cl_2 \cdot 7H_2O$, $Fe^{2+}-Y$ zeolite, and $[Fe(bpy)_3]^{2+}$/zeolite are shown in Figure 7. The spectrum of $[Fe(bpy)_3]Cl_2 \cdot 7H_2O$ (Figure 7a) gives bands at 735 and 779 cm^{-1} assigned to the deformation of the pyridine ring in the ligand and the out-of-plane C−H bending around the pyridine ring,[48] respectively. In the spectrum of $[Fe(bpy)_3]^{2+}$/zeolite (Figure 7b), a band coming from the deformation appears at ∼730 cm^{-1} and that from the C−H bending shifts to ∼ 760 cm^{-1} over the absorption arising from the zeolite lattice. Figure 8 indicates a subtraction spectrum of $[Fe(bpy)_3]^{2+}$/zeolite (Figure 7b−7c) in the 700−800 cm^{-1} region, in which both of the two bands split, as indicated in the figure. The splitting of the bands may support the expectation from the proposed model that the pyridine rings in each of the ligands of $[Fe(bpy)_3]^{2+}$ in the supercage are located under different conditions.

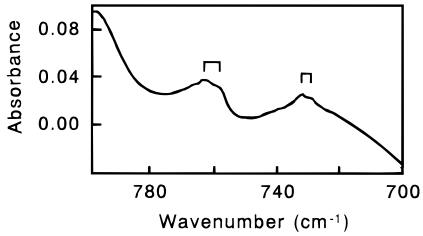

Figure 8. Subtraction spectrum of $[Fe(bpy)_3]^{2+}$/zeolite (Figure 7b−7c).

The twisting around the 3-fold axis of $[Fe(bpy)_3]^{2+}$ or $[Fe(phen)_3]^{2+}$ should bring about a large electric-field gradient at the iron nucleus in the complex ion. This may cause extraordinarily large QS values, as observed in the Mössbauer spectra of $[Fe(bpy)_3]^{2+}$/zeolite and $[Fe(phen)_3]^{2+}$/zeolite. A point-charge model calculation supports the idea that the twisting around the 3-fold axis from an octahedron toward a trigonal prism may give rise to the observed large QS values in the spectra of $[Fe(bpy)_3]^{2+}$/zeolite and $[Fe(phen)_3]^{2+}$/zeolite.

Conclusions

A series of Fe^{2+} complex ions have been prepared in the supercage of zeolite Y in order to investigate the structural change by the interaction between the complex ions and the zeolite lattice. According to the size and structure of the complex ions, $[Fe(en)_3]^{2+}$ and $[Fe(amp)_3]^{2+}$ exist undistortedly in the supercage, $[Fe(bpy)_3]^{2+}$ and $[Fe(phen)_3]^{2+}$ in the cage are largely distorted by the zeolite lattice, whereas $[Fe(dmbpy)_3]^{2+}$ and $[Fe(dmphen)_3]^{2+}$ cannot be encapsulated in zeolite Y.

As for $[Fe(bpy)_3]^{2+}$ and $[Fe(phen)_3]^{2+}$, each complex ion is located in the supercage with its 3-fold axis parallel to that of the supercage; each of the three ligands faces to the 12-membered ring of the supercage. These complexes are twisted around their 3-fold axes from an octahedron to a trigonal prism.

The conclusions may be extended over 6-coordinated complexes, even outside the Fe^{2+} complexes studied in this work, formed in the faujasite-type zeolite.

References and Notes

(1) Ozin, G. A.; Gil, C. *Chem. Rev.* **1989**, *89*, 1749.
(2) Herron, N. *CHEMTECH* **1989**, 542.
(3) Turbevill, W.; Robins, D. S.; Dutta, P. K. *J. Phys. Chem.* **1992**, *96*, 5024.
(4) Quayle, W. H.; Lunsford, J. H. *Inorg. Chem.* **1982**, *21*, 97.
(5) Quayle, W. H.; Peeters, G.; DeRoy, G. L.; Vansant, E. F.; Lunsford, J. H. *Inorg. Chem.* **1982**, *21*, 2226.
(6) Titiloye, J. O.; Parker, S. C.; Stone, F. S.; Catlow, C. R. A. *J. Phys. Chem.* **1991**, 95, 4038.
(7) Czjzek, M.; Fuess, H.; Vogt, T. *J. Phys. Chem.* **1991**, *95*, 5255.
(8) Steele, M. R.; MacDonald, P. M.; Ozin, G. A. *J. Am. Chem. Soc.* **1993**, *115*, 7285.
(9) Sun, T.; Seff, K. *J. Phys. Chem.* **1993**, *97*, 5213.
(10) Jelinek, R.; Özkar, S.; Pastore, H. O. Malek, A.; Ozin, G. A. *J. Am. Chem. Soc.* **1993**, *115*, 563.
(11) Brémard, C.; Ginestet, G.; Laureyns, J.; Maire, M. L. *J. Am. Chem. Soc.* **1995**, 117, 9274.
(12) Schrimpf, G.; Tavitian, B.; Espinat, D. *J. Phys. Chem.* **1995**, *99*, 10932.
(13) Yamashita, H.; Matsuoka, M.; Tsuji, K.; Shioya, Y.; Anpo, M.; Che, M. *J. Phys. Chem.* **1996**, *100*, 397.

(14) Shah, R.; Gale, J. D.; Payne, M. C. *J. Phys. Chem.* **1996**, *100*, 11688.
(15) Bates, S. P.; van Well, W. J. M.; van Santen, R. A.; Smit, B. *J. Am. Chem. Soc.* **1996**, *118*, 6753.
(16) Cano, M. L.; Corma, A.; Fornés, V.; García, H.; Miranda, M. A.; Baerlocher, C.; Lengauer, C. *J. Am. Chem. Soc.* **1996**, *118*, 11006.
(17) Grey, C. P.; Poshni, F. I.; Gualtieri, A. F.; Norby, P.; Hanson, J. C.; Corbin, D. R. *J. Am. Chem. Soc.* **1997**, *119*, 1981.
(18) Yeom, Y. H.; Kim, Y.; Song, S. H.; Seff, K. *J. Phys. Chem. B* **1997**, *101*, 2138.
(19) Jang, S. B.; Jeong, M. S.; Kim, Y.; Seff, K. *J. Phys. Chem. B* **1997**, *101*, 3091.
(20) Weckhuysen, B. M.; Verberckmoes, A. A.; Fu, L.; Schoonheydt, R. A. *J. Phys. Chem.* **1996**, *100*, 9456.
(21) Umemura, Y.; Minai, Y.; Tominaga, T. *J. Radioanal. Nucl. Chem. Lett.* **1994**, *186*, 213.
(22) Knops-Gerrits, P. P.; De Vos, D.; Thibault-Starzyk, F.; Jacobs, P. A. *Nature* **1994**, *369*, 543.
(23) Knops-Gerrits, P. P.; De Vos, D. E.; Jacobs, P. A. *J. Mol. Catal. A* **1997**, *117*, 57.
(24) Maruszewski, K.; Strommen, D. P.; Handrich, K.; Kincaid, J. R. *Inorg. Chem.* **1991**, *30*, 4579.
(25) Maruszewski, K.; Strommen, D. P.; K.; Kincaid, J. R. *J. Am. Chem. Soc.* **1993**, *115*, 8345.
(26) Ledney, M.; Dutta, P. K. *J. Am. Chem. Soc.* **1995**, *117*, 7687.
(27) Lainé, P.; Lanz, M.; Calzaferri, G. *Inorg. Chem.* **1996**, *35*, 3514.
(28) Herron, N. *Inorg. Chem.* **1986**, *25*, 4714.
(29) Bedioui, F.; De Boysson, E.; Devynck, J.; Balkus Jr., K. J. *J. Chem. Soc., Faraday Trans.* **1991**, *87*, 3831.
(30) Senaratne, C.; Zhang, J.; Baker, M. D.; Bessel, C. A.; Rolison, D. R. *J. Phys. Chem.* **1996**, *100*, 5849.
(31) Bessel, C. A.; Rolison, D. R. *J. Phys. Chem. B* **1997**, *101*, 1148.
(32) Delgass, W. N.; Garten, R. L.; Boudart, M. *J. Phys. Chem.* **1969**, *73*, 2970.
(33) Garten, R. L.; Delgass, W. N.; Boudart, M. *J. Catal.* **1970**, *18*, 90.
(34) Petrera, M.; Gennaro, A.; Gherardi, P.; Gubitosa, G.; Pernicone, N. *J. Chem. Soc., Faraday Trans. 1* **1984**, *80*, 709.
(35) de Bont, P. W.; Vissenberg, M. J.; Boellaard, E.; de Beer, V. H. J.; Rob van Veen, J. A.; van Santen, R. A.; van der Kraan, A. M. *J. Phys. Chem. B* **1997**, *101*, 3072.
(36) Umemura, Y.; Minai, Y.; Tominaga, T. *J. Chem. Soc., Chem. Commun.* **1993**, 1822.
(37) Breuil, M. R. E. *C. R. Acad. Sci.* **1933**, *196*, 2009.
(38) Chum, H. L.; Vanin, J. A.; Holanda, M. I. D. *Inorg. Chem.* **1982**, *21*, 1146.
(39) Akabori, K.; Matsuo, H.; Yamamoto, Y. *J. Inorg. Nucl. Chem.* **1973**, 35, 2679.
(40) Greenaway, A. M.; O'connor, C. J.; Schrock, A.; Sinn, E. *Inorg. Chem.* **1979**, 18, 2692.
(41) Katz, B. A.; Strouse, C. E. *Inorg. Chem.* **1980**, *19*, 658.
(42) Beattie, J. K. *Adv. Inorg. Chem.* **1988**, *32*, 1.
(43) Jakobi, R.; Spiering, H.; Wiehl, L.; Gmelin, E.; Gütlich, P. *Inorg. Chem.* **1988**, *27*, 1823.
(44) Umemura, Y.; Minai, Y.; Tominaga, T. *J. Chem. Soc., Chem. Commun.* **1994**, 893.
(45) Niven, M. L.; Percy, G. C.; Thornton, D. A. *J. Mol. Struct.* **1980**, *68*, 73.
(46) Champion, A. R.; Vaughan, R. W.; Drickamer, H. G. *J. Chem. Phys.* **1967**, *47*, 2583.
(47) Champion, A. R.; Drickamer, H. G. *J. Chem. Phys.* **1967**, *47*, 2591.
(48) Altmann, W.; Perkampus, H. H. *Spectrochim. Acta* **1979**, *35A*, 253.